Factors Contributing to the Summer 2003 European Heatwave

Emily Black, Mike Blackburn, Giles Harrison, Brian Hoskins and John Methven
Department of Meteorology, University of Reading, UK

European temperature record

Europe was exceptionally warm and dry from May through to the end of August 2003. Figure 1 shows the European average surface air temperature (at 2m) derived from global analyses of the European Centre for Medium-range Weather Forecasts (ECMWF). The analyses are calculated for every 6 hour period at 00, 06, 12 and 18UTC. The daily average is also shown for comparison with the daily climatology for 1958-2002 obtained from the ECMWF re-analysis project (ERA-40; Simmons and Gibson, 2000). The heatwaves in June and early August can readily be identified. During these periods even the night-time temperatures exceeded the climatological daily averages! Averaging over each month, Fig. 7 below shows that the temperature anomalies were 4.2°C in June, 3.8°C in August and almost 2°C in May and July. The temperature anomalies were most extreme in France and Switzerland although maximum temperature records were broken in many parts of Europe. For example, Schär et al (2004) have shown that the June-July-August (JJA) temperature averaged for four Swiss stations exceeded the 1864-2000 mean by 5.1°C, far greater than the next highest anomaly of 2.7°C in 1947. Both Beniston (2004) and Schär et al (2004) argue that a repeat of the 2003 summer would be extremely unlikely if stationarity in the past statistics were to be assumed, but that the temperatures experienced across Europe in summer 2003 could be considered "normal" by the end of the 21st century under a high greenhouse-gas emissions scenario. Given the increased human mortality experienced during the 2003 heatwave (WHO, 2003; Kovats et al, 2004), this has important implications for future human health.

Here we attempt to draw together the factors that may have contributed to this exceptional summer by examining the large-scale atmospheric flow and the regional heat budget from ECMWF analyses and measurements of the surface energy budget at Reading. The influence of atmospheric flow anomalies on the surface of the land and ocean and possible feedbacks are also discussed.

Atmospheric flow anomalies in the Northern Hemisphere

Figure 2 shows monthly anomalies of low level (850hPa) streamfunction for May to August 2003. Europe was dominated by anomalous anticyclonic conditions (high values of streamfunction) throughout the period, beginning in May with a marked northward displacement of the subtropical Azores anticyclone, extending from the mid-Atlantic through to eastern Europe, and a general strengthening of westerly flow on its poleward flank over the UK and southern Scandinavia. For each of the subsequent summer months, a pattern of anomalies persisted over the Atlantic sector, comprising low (cyclonic) streamfunction values over the northern coast of south America, high (anticyclonic) values northeast of the Caribbean, low values in the central or northeast Atlantic and high values over continental Europe. During May, June and August there was also an obvious train of anomalies (low-

high-low streamfunction) extending across Russia to the Pacific coast. This pattern is also seen along 45°N during July, although a much stronger anticyclonic anomaly extended across Scandinavia to the Urals. The European anomaly varied through the summer, being stronger and with more anticyclonic curvature in June and August, and weaker in July. The cyclonic anomaly over the Atlantic was situated west of the UK in June and July and further southwest in August. Throughout the four-month period, the anomalous flow over the UK contained a southerly component, but it gradually turned from being southwesterly with cyclonic curvature in May to being southeasterly with anticyclonic curvature in August. This indicates an increasing tendency to advect air at low-levels over the UK from continental Europe rather than from the Atlantic.

The large-scale anomalies at mid-tropospheric levels (Grazzini et al, 2003) were very similar to those just described at low levels, indicating an approximately equivalent barotropic vertical structure on monthly timescales. The streamfunction pattern of alternating signed anomalies from South America to Europe and beyond is suggestive of a Rossby wave signal propagating from tropical America.

Influence of flow anomalies on radiative fluxes and sea surface temperature

The observed top-of-atmosphere (TOA) outgoing long-wave radiation (OLR) anomalies for June-August 2003 (Fig. 3) show increased OLR over Europe, associated with reduced cloud and precipitation (NOAA, 2003) in the region of the anticyclonic anomaly. Over the North Atlantic, the OLR anomalies show a pattern with five zonal bands. Looking northwards from the equator, there was a high-low dipole straddling the climatological latitude (8-9°N) of the West African Inter-Tropical Convergence Zone (ITCZ). This resulted from a northward shift and regional intensification of the ITCZ - throughout the rest of the tropics, apart from the NW Indian Ocean, the ITCZ was weaker than normal (not shown here). The next band (anomalously high OLR) is associated with an intensification of the Azores anticyclone. At the same time, the Icelandic Low was further south than normal, associated with enhanced cyclonic activity south of Iceland and reduced cyclonic activity to the north of 60°N. The TOA net radiative fluxes from ECMWF 0-24 hour forecasts (not shown) also possess the same banded pattern, with anomalously large downward fluxes in the strip stretching across the Atlantic WSW of Portugal and reduced fluxes to the north and south. The same pattern is also seen in the net radiative fluxes at the surface but with reduced amplitude. Taken together the fluxes are indicative over the North Atlantic of reduced cloud to the WSW of Portugal and increased cloud to the north and south of this strip, which are associated with intensification of the Azores Anticyclone, a northward shift in the ITCZ and a southward shift in the summer extratropical stormtrack.

Figure 4 shows the evolution of sea surface temperature (SST) anomalies between May and August. At the end of April and early May, the Mediterranean warmed rapidly (the SST anomalies were less than 0.5K on average during April). In the East Atlantic a banded pattern emerged with five distinct centres: anomalously warm SST to the south of the ITCZ, cold on its northern flank, warm SST to the WSW of Portugal, cold SST between Ireland and Newfoundland and warm SST poleward of 60°N. In June, both the warmth of the Mediterranean and the pattern in the East Atlantic intensified. During July, the unusually warm Mediterranean SST persisted with record breaking temperatures exceeding 30°C (Grazzini et al, 2003) while the air temperature over Europe was less anomalous. In the Atlantic the warm SST to the WSW of Portugal and the cold SST to the west of Ireland further intensified and the warm SSTs off the Norwegian coast became especially strong

2

under the clear skies associated with the anticylonic anomaly centred over Scandinavia (Fig. 2). The Atlantic banded pattern in radiative fluxes was particularly strong in May but weak in July. In contrast, the SST pattern amplified most rapidly between May and June and hardly changed between July and August, suggesting that the SST anomalies responded passively to the radiative flux anomalies.

Globally, the strongest OLR anomaly ($< -30Wm^{-2}$) during this period was situated above anomalously high SST in the NW Indian Ocean. This SST anomaly (Fig. 4) was located off the coast of Somalia in May, moving north to the Arabian Sea by July. It was strongest in June (above 1.5°C) and may have been associated with the late onset of the Asian Summer monsoon in 2003, a weaker Somali Jet in the lower troposphere along the East African coast and weaker upwelling of cold water. Rodwell and Hoskins (1996) have demonstrated that the atmospheric response to heating in the monsoon region includes enhanced descent over the Eastern Mediterranean. This strong descent keeps the air above the Mediterranean particularly dry and suppresses convection, resulting in the hot and dry Mediterranean summer climate. However, the late monsoon onset in 2003 cannot account for the exceptionally hot and dry conditions over Europe in May and June. Possible teleconnections relating the European summer to anomalies further afield include the overall intensification of the Azores High and northward shift of the West African ITCZ, and the Rossby wave signal from tropical America.

Steady anticyclone and descending air over Western Europe

The most extreme temperatures in Western Europe were experienced from 6-12th August. During this period there were very slack gradients in mean sea level pressure but there was a weak signature of blocking, with a high over the UK and North Sea, a low over Iberia and a high over the Western Mediterranean (see *Weather Log* - corrected maps for August 2003 came with the November issue of *Weather*). The blocking system was centred over Northern France. Figure 5 shows 7-day trajectories calculated backwards in time using the UGAMP trajectory model (Methven, 1997) from a point 500m above Paris every 6 hours during this period. The steadiness of the anticyclone had the result that air was trapped within it and travelled a very short distance (compared with typical trajectories for the European sector) during the week preceding arrival. While caught in the anticyclone, the trajectories generally descended.

Above the top of the daytime boundary layer (BL) air masses experienced cooling at a steady rate, as seen by the change in potential temperature following trajectories (Fig. 6a) that arrived at 18:00 UTC 12th August (the hottest day in Paris reaching 40.0°C). Potential temperature takes account of adiabatic compression of unsaturated air parcels so that its value would be constant along 3D trajectories in the absence of heat exchange: the calculation is sufficiently accurate that changes greater than 1K can be related to diabatic heating or cooling (Methven *et al*, 2003). The potential temperature decrease is indicative of radiative cooling to space in the clear air within the anticyclone (at a rate of about -2 K/day). The cooling enabled steady descent across isentropic surfaces in the stably stratified free troposphere. Note that the two trajectories that arrived at the top of the profile had experienced strong heating between 10 and 6 days ago. This did not occur over Europe but within a warm conveyor belt - a body of air that condensed water vapour and released latent heat as it ascended following the US East Coast to Newfoundland. The remaining trajectories circled anticyclonically around Europe.

During the heatwave the surface was heated strongly and turbulence and dry convection (i.e., without condensation) enabled the BL to extend much higher than normal. The red curves in Fig. 6b show profiles at 18:00 UTC above Paris derived from ECMWF analyses - virtual potential temperature[1] was mixed throughout the BL from the ground up to about 4km by late afternoon, resulting in an almost adiabatic (convectively neutral) profile. The atmosphere was only out of direct contact with the ground above 4 km or for potential temperatures greater than 314K. It is clear from Fig. 6a that radiative cooling occurred above 314K but that potential temperature remained fairly constant following trajectories in the adiabatic layer, presumably because turbulent mixing from the hot surface overcame the cooling. At night the surface cooled rapidly, resulting in a very stable nocturnal boundary layer up to about 500m as seen in the 06:00 UTC profiles (black curves in Fig. 6b). Above this the residual adiabatic layer remained. The red-orange trajectories in Fig. 6a stay below 500m and therefore show the strong diurnal variation within the BL associated with the surface heat budget and gradual warming as the hottest day was approached.

Given the extreme surface temperatures and high relative humidity in the BL in the morning (not shown) it is perhaps surprising that moist convection, associated with condensation in ascending air and cloud formation, was not widespread during this period. However, the strong radiative cooling and descent would tend to suppress convection, thus maintaining clear sky conditions.

Heat budget for the atmosphere above Europe

Since the flow was almost stagnant, hot air was not brought into Europe from further afield. The regional heat budget must have enabled the extremely high temperatures to occur.

The impact of the anomalous anticyclonic flow and clear sky conditions is evident in estimates of the components of the top-of-atmosphere (TOA) and surface energy budget over continental Europe. We have used data for 2003 from short-term (0-24 hour) forecasts of the operational ECMWF model, and anomalies have been computed relative to the equivalent ERA-40 climatological data for the period 1958-2002. These are model products rather than directly analysed data, and they could be contaminated by any model spin-up in the 0-24 hour forecast period and by any differences between the ERA-40 version of the model and the version that was operational in summer 2003. It is difficult to estimate the size of such errors, but the data have the advantage of being spatially comprehensive and consistent with the initial evolution of the ECMWF model forecasts, which are strongly constrained by the analysed initial state.

Monthly anomalies of the energy budget averaged over European land areas within the domain 0-20ºE, 42.5-52.5ºN (shaded in Fig. 1) are shown in Figure 7. In each of the four months there was a positive (downward) net radiative flux anomaly at the top-of-atmosphere (red bars), tending to heat the land and atmospheric column, which ranged from approximately $10Wm^{-2}$ in May to $20Wm^{-2}$ in June[2]. The short-wave and long-wave components of this signal (not shown) are consistent with reduced cloud cover, namely a positive OLR anomaly in each month which was more than compensated by a reduction in reflected short-wave. Figure 7 implies that less than half of this anomalous radiative forcing

---

[1]Virtual potential temperature takes account of the lower density of moist air compared with dry air (at the same pressure and temperature) - whenever it decreases with height the atmosphere is convectively unstable.
[2] An unbalanced TOA flux anomaly of $10Wm^{-2}$ is equivalent to a heating rate of 2.5K/month in either the entire atmospheric column or in 2.5m of an ocean surface layer.

was used to heat the atmospheric column, so that more than half was available at the land surface (purple bars). On a monthly timescale, the increased surface radiative forcing was approximately balanced by increased (upward) turbulent fluxes (blue bars). The flux anomalies in June were remarkable, with almost the entire 20Wm^{-2} TOA forcing anomaly available at the surface and balanced by the turbulent flux anomaly. Notably, the seasonal evolution of the sensible and latent heat flux components was quite different: the latent heat flux anomaly (SLHF) was initially positive but became increasingly negative, indicative of a gradual drying of the land surface through the summer, whereas the sensible heat flux anomaly (SSHF) remained positive and increased, associated with increasing surface temperatures. Moreover, the energy budget clearly shows that the negative latent heat flux anomalies associated with soil drying acted to amplify the surface radiative forcing in July and August, doubling the (relatively weak) 4Wm^{-2} radiative anomaly in July and increasing the stronger August anomaly by almost 80%.

Detailed observations of the surface energy budget at Reading

The ECMWF model indicates the importance of the land surface in the gradual development of higher air temperatures over Europe. This process is further investigated by analysing measurements of temperatures, humidity and surface energy fluxes which were obtained during August 2003 using automated instruments[3] at the Department of Meteorology's field site (situated on the University of Reading's Whiteknights campus).

Two platinum resistance thermometer sensors to BS1904 (Class A), were housed in a Casella double-louvered single size Stevenson Screen, with one temperature sensor operated as a wet bulb. The resistance changes were converted to voltages using a stable linearised Wheatstone bridge circuit (Harrison and Pedder, 2001). Both temperature sensors had previous been individually calibrated in a water bath, using an ASL F25 platinum resistance thermometer traceable to national standards. Global and diffuse solar irradiances S_g and S_d were measured using two Kipp and Zonen CM5 solarimeters. The net radiative flux R_n and ground heat flux G were determined using a Kipp and Zonen NR-LITE radiometer and a McVan HP3 sensor respectively. For S_g, S_d, R_n and G, high gain thermally-stable amplifiers were used to amplify the microvolt sensor signals to high level signals for a 12 bit analogue to digital converter. The high level signals were recorded as 5minute averages derived from 1Hz samples, as described by Aplin and Harrison (2003).

As well as automatic readings, manual observations are taken at 0900UT at Reading with thermometers in a double size Stevenson Screen. Table 1 shows a summary of the observations obtained during August 2003. The maximum temperature of 36.4°C on Sunday 10th August was the highest temperature since the record began on 1st Jan 1968. Two of the four daily maximum temperatures of 34.0°C or greater occurring since the beginning of the Reading records were in August 2003: the others were on 26th June 1976 (34.0°C) and 3rd August 1990 (35.5°C).

Figure 8 shows the Reading temperature time series for 3rd to 12th August 2003. For days 219 to 222 (see Table 1 for dates), there was a rapid rise in the maximum temperatures, which generally occurred in the mid or late afternoons. The minimum nocturnal temperatures for each of the preceding nights were relatively constant, with the air cooling briefly to its dew point. On the 10th August, the maximum temperature was reached earlier (at 14:10) than

---

[3] http://www.met.rdg.ac.uk/~fsdata/metsite.html

on the previous three days, following a more rapid rise in temperature during the morning. The actual diurnal variation for 10th August 2003 is given in Fig. 9, which shows the 5 minute average values of air temperature, diffuse and global solar irradiances, the net radiation and ground heat fluxes. A small amount of cloud between 14:30 and 15:45, associated with a cloud band marked as an upper level trough ahead of a cold front in the Met Office surface analysis (see *Weather Log*), probably prevented a higher maximum temperature from occurring.

The nocturnal ground heat flux (G) is also shown in Fig. 8. It is clear that -G (which is a measure of heat leaving the soil) increased steadily from days 217 to 222, although there was no associated change in minimum air temperature. Note that during the night preceding the hottest day (10th August), G became more negative until, by dawn, it balanced the net radiation which was almost steady throughout the night (Fig. 9). The increasing cancellation of radiative cooling by the ground heat flux slowed the nocturnal decrease in surface air temperature, having a significant impact in elevating the minimum air temperature because of the shallow nocturnal boundary layer (evident for Paris in Fig. 6b). For example, an upward ground heat flux of 10Wm^{-2} would heat a 100 metre atmospheric layer at around 0.3K/hour. The maximum in the nocturnal heat flux (just over 30Wm^{-2}) was in the early hours of 10th August (day 222). The heat leaving the dry soil contributed to the rather rapid rise in temperature during the morning.

Conclusions

The extreme temperatures and lack of precipitation in Europe from May to August 2003 were related to persistent anticyclonic conditions throughout the period. In particular, during May the Azores Anticyclone and West African ITCZ were both displaced to the north while the summer stormtrack was concentrated further south than normal, resulting in a pattern with five zonal bands in cloud and radiative forcing anomalies over the East Atlantic sector, both at the surface and top of the atmosphere. The anomalously clear skies and downward net radiative fluxes led to warm SSTs in a strip extending to the WSW of Portugal (with flanking cold SST anomalies to the north and south). It also contributed to a strong loss of moisture from the European land surface. During June, although the anomalous high was much weaker over the Atlantic, it persisted over Europe resulting in extremely strong radiative anomalies, heating of the land surface and enhanced latent and sensible heat fluxes into the atmosphere which together almost balanced the radiative anomalies. The land surface warmed and dried to such an extent that, during July, when the radiative forcing was weaker, the latent heat fluxes were anomalously negative, due to lack of soil moisture, and the sensible heat fluxes were higher than usual due to the higher surface temperatures. In August a blocking regime resumed over Europe, the absence of clouds again enhanced the radiative forcing and the temperature increase at the surface was exacerbated by the inability of latent heat fluxes to transfer heat upwards due to the lack of moisture availability. Surface heat balance was almost achieved by the increase in sensible heat fluxes from the extremely hot land surface.

Observations taken at the University of Reading indicate that the ground played an important role in the accumulation of heat during the day and its gradual release at night. This acted to offset night-time cooling driven by upward longwave radiation under clear skies, slowing the decrease in air temperature before sunrise. The impact on surface air temperature was more significant because the nocturnal boundary layer was very shallow in anticyclonic conditions.

Therefore, the strong ground heat flux contributed to exceptionally warm nights, sustaining the thermal stress which led to the increased human mortality across Europe (WHO, 2003).

At Reading the record-breaking temperature on the 10th August could have been higher had cloud not passed over the area at about 14:30 UTC. Examination of satellite images (not shown) reveals that this cloud was part of a band ahead of a weak cold front which progressed very slowly across England during the 11th and 12th August towards France. The highest temperature in Paris was recorded on 12th August and the temperatures fell by 6°C the next day, heralding the end of the most severe heatwave ever experienced in Europe.

In summer 2003 the large-scale atmospheric circulation enabled a dominance of the local heat balance over Europe under clear skies and with an increasingly dry land surface: the result was the exceptionally high temperatures. It is not known at this time why the large-scale circulation had the character it did.

Acknowledgements

References

Aplin, K.L. and Harrison, R.G. (2003) Meteorological effects of the eclipse of 11th August 1999 in cloudy and clear conditions. *Proc Roy Soc Lond* A, **459**, 2030, 353-372. (10.1098/rspa.2002.1042)

Beniston, M. (2004) The 2003 heat wave in Europe: A shape of things to come? An analysis based on Swiss climatological data and model simulations. *Geophys. Res. Lett.*, **31**, 2022-2026.

Grazzini, F., Ferranti, L., Lalaurette, F. and Vitard, F. (2003) The exceptional warm anomalies of summer 2003. *ECMWF Newsletter*, No 99, 2-8.

Harrison, R.G. and Pedder, M.A. (2001) Fine wire thermometer for air temperature measurement *Rev Sci Inst*, **72**, 2, 1539-1541.

Kovats, S., Wolf, T. and Menne, B. (2004) Heatwave of August 2003 in Europe: provisional estimates of the impact on mortality. *Eurosurveillance Weekly*, **8**(11), 11 March 2004. (http://www.eurosurveillance.org/ew/2004/040311.asp#7).

Methven, J. (1997) Offline trajectories: Calculation and accuracy. *Tech. Report 44*, U.K. Univ. Global Atmos. Modelling Programme, Dept. of Meteorol., Univ. of Reading, Reading, U.K.

Methven, J., Arnold, S.R., O'Connor, F.M., Barjat, H., Dewey, K., Kent, J. and Brough, N. (2003) Estimating photochemically produced ozone throughout a domain using flight data and a Lagrangian model. *J. Geophys. Res.*, **108**(D9), 4271, doi:10.1029/2002JD002955.

NOAA (2003) *Climate Diagnostics Bulletin*. Available from: Climate Prediction Center, Camp Springs, Maryland, USA (monthly). Nos. 03/6-8. (http://www.cpc.ncep.noaa.gov/products/analysis_monitoring/CDB_archive.html).

Rodwell, M. R. and Hoskins, B. J. (1996) Monsoons and the dynamics of deserts. *Quart. J. Roy. Met. Soc.,* **122**, 1385-1404.

Schär, C., Vidale, P.L., Lüthi, D., Frei, C., Häberli, C., Li niger, M.A. and Appenzeller, C. (2004) The role of increasing temperature variability in European summer heatwaves. *Nature*, **427**, 332-336.

Simmons, A.J. and Gibson, J.K. (2000) The ERA -40 Project Plan, *ERA-40 Project Report Series No. 1*, ECMWF, Reading, RG2 9AX, UK, 63pp.

WHO (2003) Heatwaves: impacts and responses. Information note for the 9th meeting of the European Environment and Health Committee of the World Health Organisation, October 2003.
12pp.

Table 1. Manual observations from Reading of daily maximum and minimum temperatures, and sunshine hours from a Campbell-Stokes instrument (09UT).

Manual Observations at Reading University Field site

Date	year day	T Max (deg)	T min (deg)	Sunshine hours (hours)
03/08/2003	215	28.1	10.4	8.9
04/08/2003	216	31.2	13.2	0.0
05/08/2003	217	31.9	18.4	13.5
06/08/2003	218	32.9	18.1	13.4
07/08/2003	219	29.2	16.5	11.2
08/08/2003	220	29.8	16.1	9.4
09/08/2003	221	34.2	16.4	13.0
10/08/2003	222	36.4	16.2	10.0
11/08/2003	223	33.3	19.9	12.4
12/08/2003	224	28.7	18.0	12.7
13/08/2003	225	27.7	15.6	11.6

Figure 1

Time series of 2 metre air temperature for summer 2003 from ECMWF operational analyses averaged over Europe (the land region shaded grey in the inset). The analyses were calculated for the regular times 00, 06, 12, 18 UTC and the daily average is also shown (dark blue line). The dashed line shows the climatology obtained by averaging the temperatures for each date over the years 1958-2002 using ERA-40 data (the land-sea mask differs very slightly from the operational one).

Figure 2

Monthly anomalies of streamfunction on the 850hPa pressure level for May-August 2003. The anomalies are deviations of the ECMWF operational analyses for 2003 from the ERA-40 climatology for 1958-2002. Shading interval 10^6 m^{2}s^{-1}.

Figure 3

NOAA satellite-observed outgoing long-wave radiation (OLR) anomalies averaged over June-August 2003, calculated as departures from the 1979-1995 climatological average. Units are Wm^{-2}.

Figure 4
Monthly mean SST anomalies (skin temperature in °C) for May to August 2003. The anomalies are calculated as the deviation of ECMWF operational analyses from the ERA-40 climatology for 1958-2001.

Figure 5
Trajectories calculated following the winds from ECMWF analyses backwards in time for 7 days from 500m above Paris, releasing one every 6 hours for the 6-12th August 2003. The bottom panel plots the longitude-height coordinates of each trajectory. The colours correspond to the "arrival time" above Paris passing from red-yellow-green-blue.

Figure 6
(a) Potential temperature following 10-day back trajectories from levels between the ground and 5km above Paris, releasing them all at 18:00UTC 12th August 2003. (b) Virtual potential temperature from the ECMWF analyses versus height for the 6-12th August 2003. Red curves are for 18UTC, black curves for 06UTC on each day.

Figure 7
Monthly anomalies in the energy budget for the European land area 0-20ºE, 42.5-52.5ºN, for May-August 2003. The bars correspond to anomalies in: TOA net radiative flux (red), surface net radiative flux (purple), surface sensible heat flux (open, orange), surface latent heat flux (open, blue) and surface turbulent flux (SHF+LHF) (blue). Data are from ECMWF short term forecasts (0-24 hours), computed as departures from the ERA-40 climatology for 1958-2002. Downward radiative fluxes and upward turbulent fluxes are positive. Monthly anomalies in 2 metre temperature are also shown (hatched).

Figure 8
Time series of automatic temperature measurements obtained at the Whiteknights campus at Reading during early August 2003 (scale on left hand axis). Nocturnal ground heat flux (*negative* values represent heat *leaving* the soil) is also shown.

Figure 9
Surface solar irradiances, net radiation and ground heat fluxes measured during August 10th 2003, at Reading. Simultaneous measurements of screen air temperature are also shown.
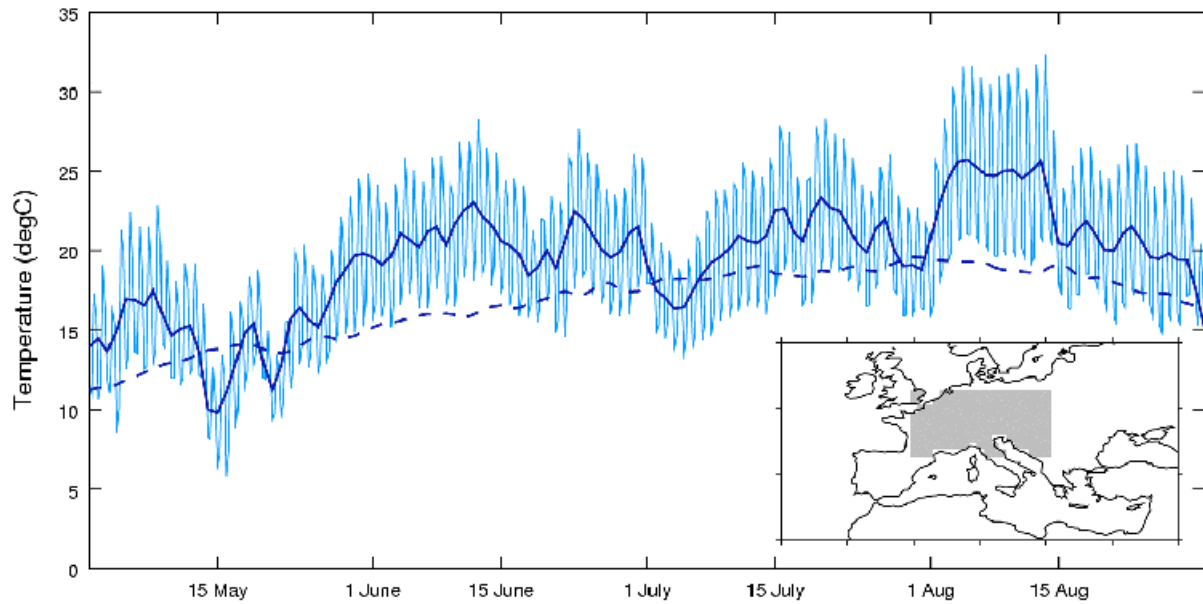
Figure 1
Time series of 2 metre air temperature for summer 2003 from ECMWF operational analyses averaged over Europe (the land region shaded grey in the inset). The analyses were calculated for the regular times 00, 06, 12, 18 UTC and the daily average is also shown (dark blue line). The dashed line shows the climatology obtained by averaging the temperatures for each date over the years 1958-2002 using ERA-40 data (the land-sea mask differs very slightly from the operational one).
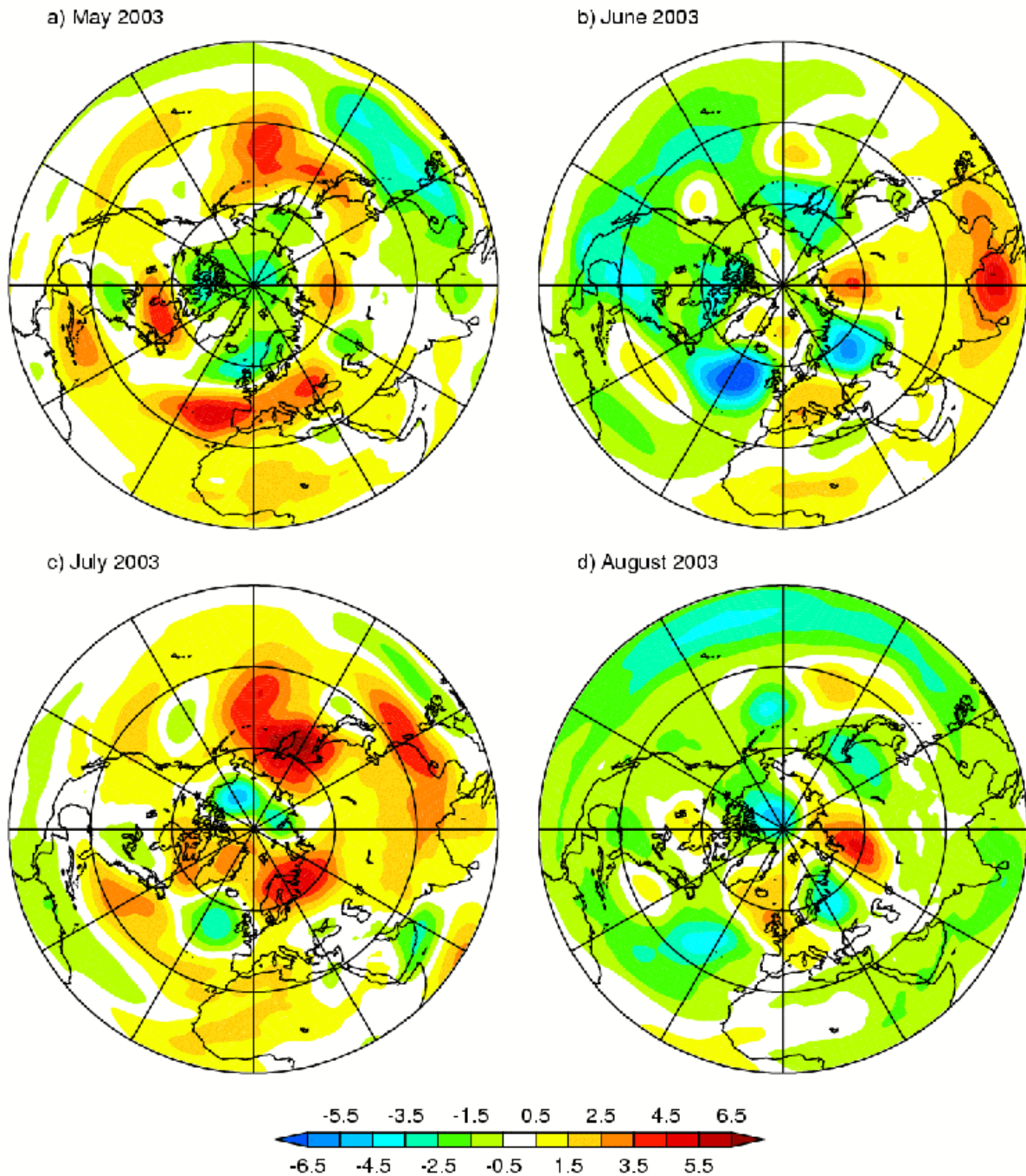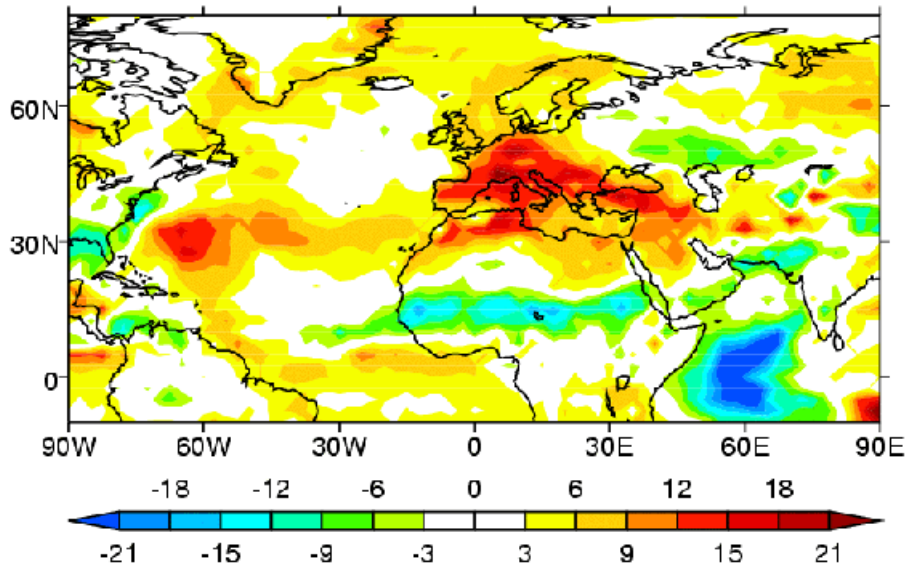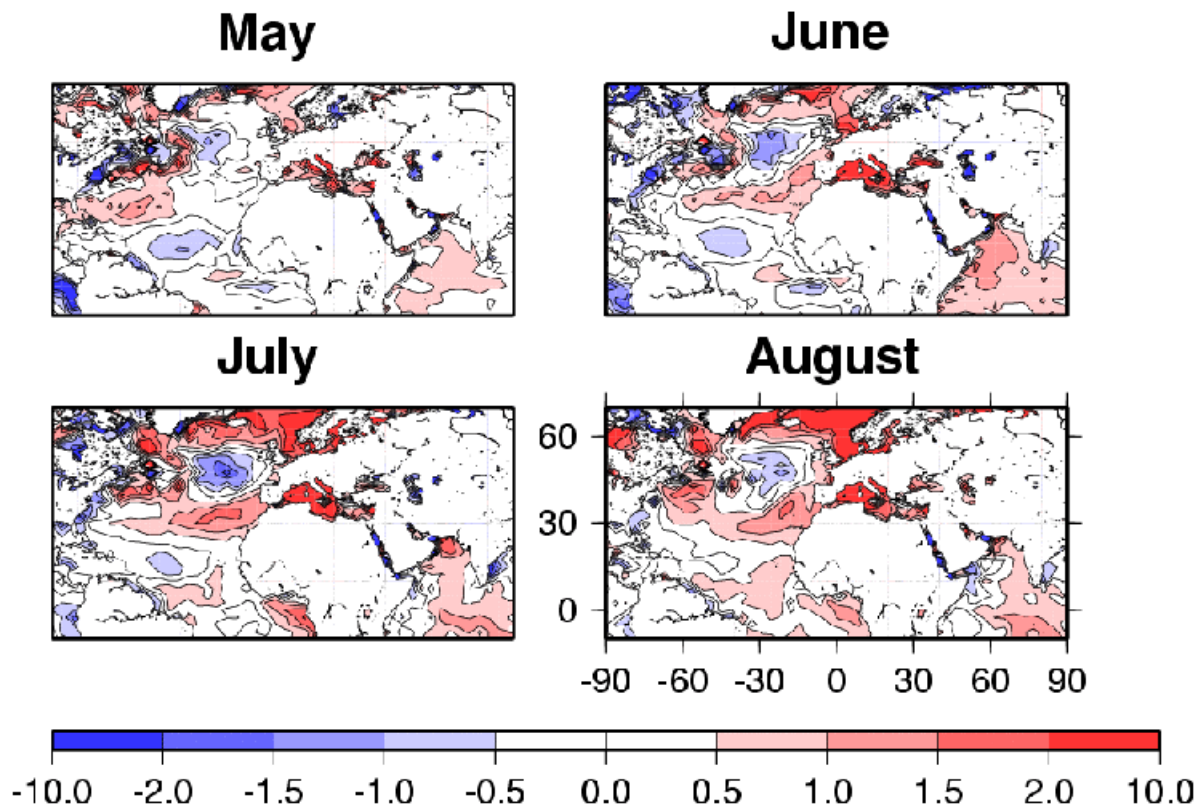
Figure 2
Monthly anomalies of streamfunction on the 850hPa pressure level for May-August 2003. The anomalies are deviations of the ECMWF operational analyses for 2003 from the ERA-40 climatology for 1958-2002. Shading interval 10^6 m^{2}s^{-1}.

Figure 3
NOAA satellite-observed outgoing long-wave radiation (OLR) anomalies averaged over June-August 2003, calculated as departures from the 1979-1995 climatological average. Units are Wm^{-2}.

Figure 4
Monthly mean SST anomalies (skin temperature in °C) for May to August 2003. The anomalies are calculated as the deviation of ECMWF operational analyses from the ERA-40 climatology for 1958-2001.

Figure 5

Trajectories calculated following the winds from ECMWF analyses backwards in time for 7 days from 500m above Paris, releasing one every 6 hours for the 6-12th August 2003. The bottom panel plots the longitude-height coordinates of each trajectory. The colours correspond to the "arrival time" above Paris passing from red-yellow-green-blue.
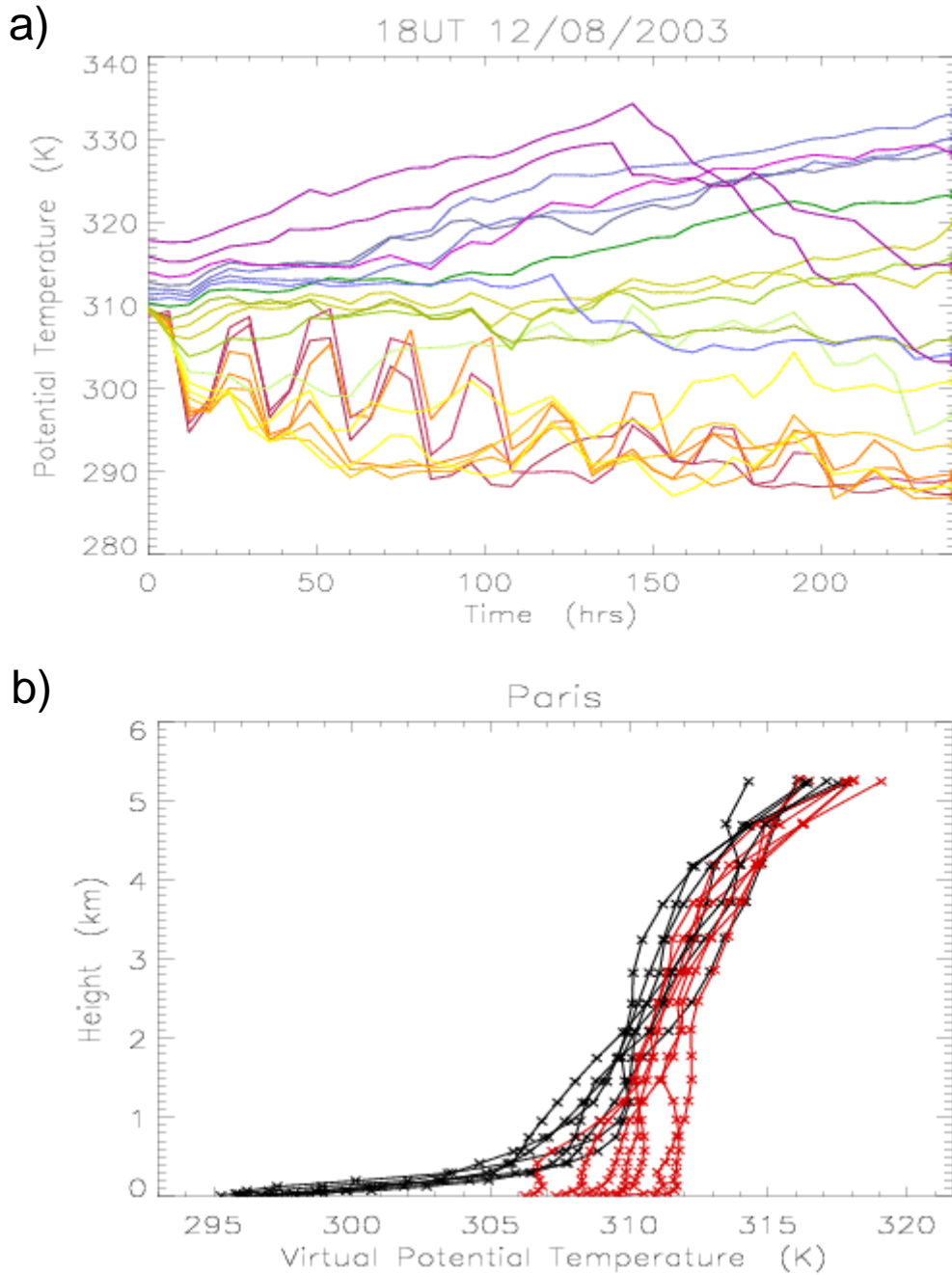
Figure 6
(a) Potential temperature following 10-day back trajectories from levels between the ground and 5km above Paris, releasing them all at 18:00UTC 12th August 2003. (b) Virtual potential temperature from the ECMWF analyses versus height for the 6-12th August 2003. Red curves are for 18UTC, black curves for 06UTC on each day.
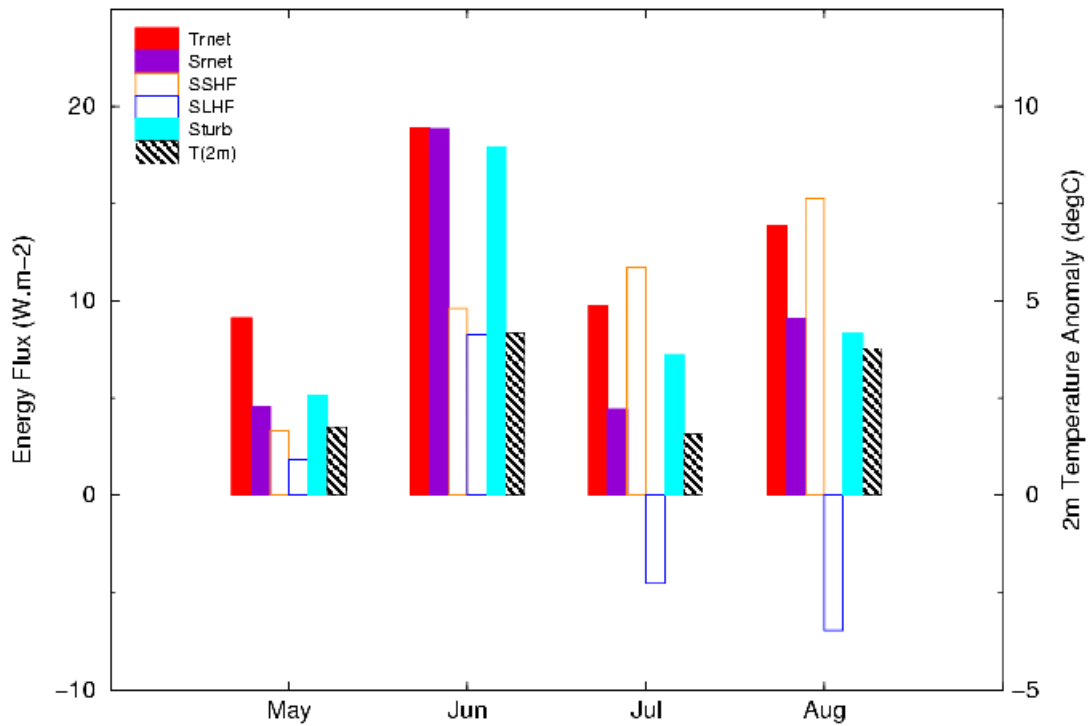
Figure 7
Monthly anomalies in the energy budget for the European land area 0-20ºE, 42.5-52.5ºN, for May-August 2003. The bars correspond to anomalies in: TOA net radiative flux (red), surface net radiative flux (purple), surface sensible heat flux (open, orange), surface latent heat flux (open, blue) and surface turbulent flux (SHF+LHF) (blue). Data are from ECMWF short term forecasts (0-24 hours), computed as departures from the ERA-40 climatology for 1958-2002. Downward radiative fluxes and upward turbulent fluxes are positive. Monthly anomalies in 2 metre temperature are also shown (hatched).
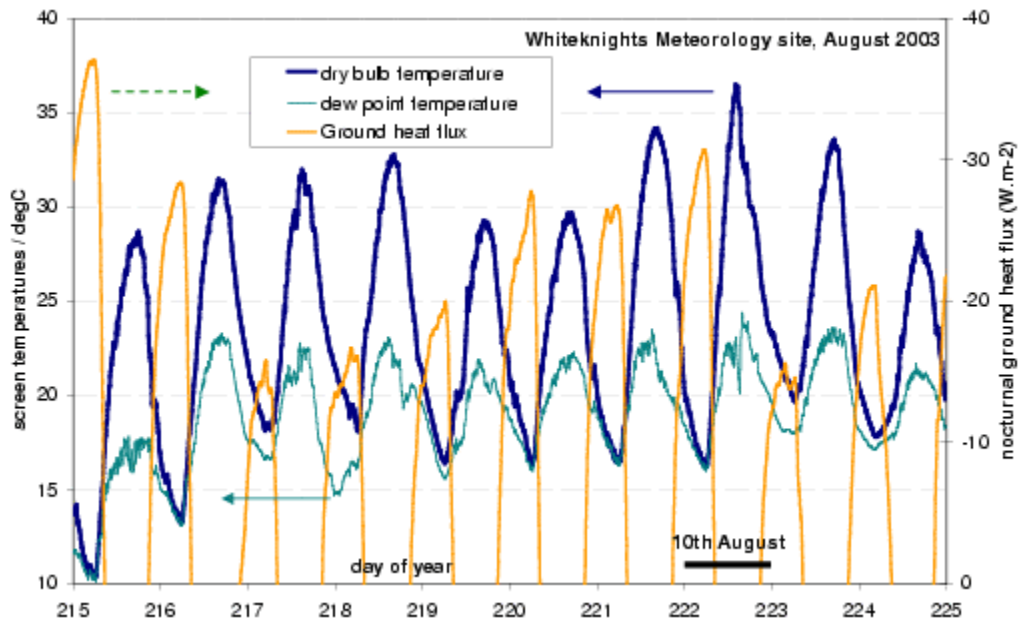
Figure 8
Time series of automatic temperature measurements obtained at the Whiteknights campus at Reading during early August 2003 (scale on left hand axis). Nocturnal ground heat flux (*negative* values represent heat *leaving* the soil) is also shown.
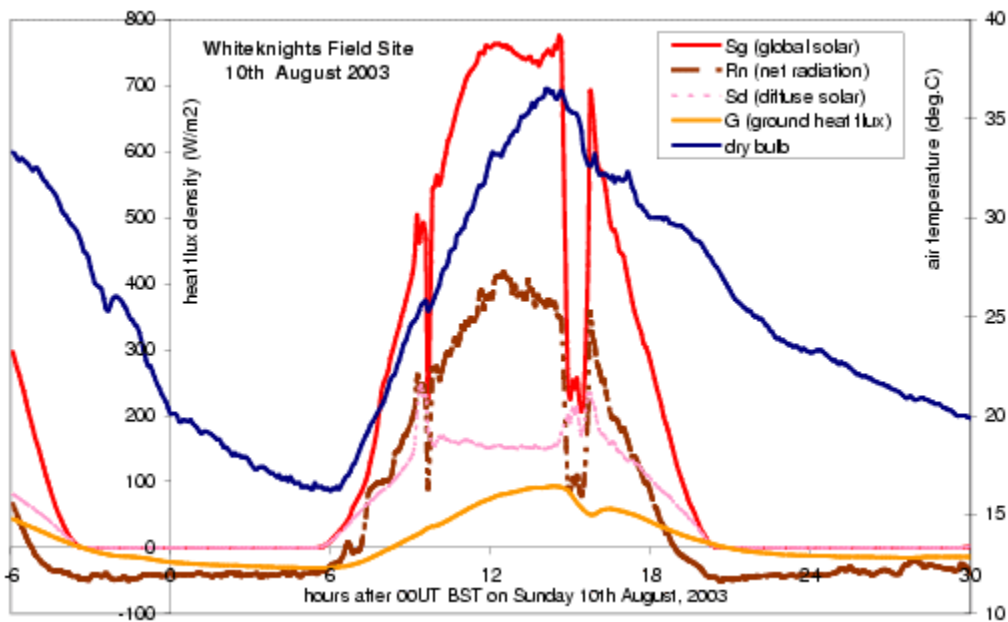

Figure 9
Surface solar irradiances, net radiation and ground heat fluxes measured during August 10th 2003, at Reading. Simultaneous measurements of screen air temperature are also shown.